DNA Vaccine Expressing the Mimotope of GD2 Ganglioside Induces Protective GD2 Cross-reactive Antibody Responses

Elizabeth Bolesta,[1] Aleksandra Kowalczyk,[1] Andrzej Wierzbicki,[1] Piotr Rotkiewicz,[3] Barbara Bambach,[2] Chun-Yen Tsao,[1] Irena Horwacik,[4] Andrzej Kolinski,[3] Hanna Rokita,[4] Martin Brecher,[2] Xinhui Wang,[1] Soldano Ferrone,[1] and Danuta Kozbor[1]

Departments of [1]Immunology and [2]Pediatrics, Roswell Park Cancer Institute, Buffalo, New York; [3]Faculty of Chemistry, Warsaw University, Warszawa, Poland; and [4]Faculty of Biotechnology, Jagiellonian University, Kraków, Poland

Abstract

The GD2 ganglioside expressed on neuroectodermally derived tumors, including neuroblastoma and melanoma, is weakly immunogenic in tumor-bearing patients and induces predominantly immunoglobulin (Ig)-M antibody responses in the immunized host. Here, we investigated whether interconversion of GD2 into a peptide mimetic form would induce GD2 cross-reactive IgG antibody responses in mice. Screening of the X_{15} phage display peptide library with the anti-GD2 monoclonal antibody (mAb) 14G2a led to isolation of mimetic peptide 47, which inhibited the binding of 14G2a antibody to GD2-positive tumor cells. The peptide was also recognized by GD2-specific serum antibodies from a patient with neuroblastoma, suggesting that it bears an internal image of GD2 ganglioside expressed on the tumor cells. The molecular basis for antigenicity of the GD2 mimetic peptide, established by molecular modeling and mutagenesis studies, led to the generation of a 47-LDA mutant with an increased mimicry to GD2. Immunization of mice with peptide 47-LDA–encoded plasmid DNA elicited GD2 cross-reactive IgG antibody responses, which were increased on subsequent boost with GD2 ganglioside. The vaccine-induced antibodies recognized GD2-positive tumor cells, mediated complement-dependent cytotoxicity, and exhibited protection against s.c. human GD2-positive melanoma growth in the severe combined immunodeficient mouse xenograft model. The results from our studies provide insights into approaches for boosting GD2 cross-reactive IgG antibody responses by minigene vaccination with a protective epitope of GD2 ganglioside. (Cancer Res 2005; 65(8): 3410-8)

Introduction

Neuroblastoma, melanoma, and sarcoma cells abundantly express the gangliosides GM2, GD2, and GD3 on the cell surface where they are susceptible to immune attack by antibodies (1, 2). The GD2 ganglioside is an especially appealing target because it is highly expressed on neuroectodermal tumor cells with limited heterogeneity (3, 4), is rarely lost following monoclonal antibody (mAb) therapy (5), and has a restricted distribution in normal tissues except for neurons, skin melanocytes, and peripheral pain fibers (6, 7). The basis for cancer vaccines targeting GD2 ganglioside that primarily elicits an antibody response has been established in both experimental models and clinical settings (8–10). A number of therapeutic trials with mAbs specific for GD2 ganglioside have shown partial *in vivo* antitumor effects in patients with neuroblastoma and malignant melanoma (11–15). Studies of a radiolabeled murine GD2-specific mAb 3F8 have revealed that the antibody does not cross the intact blood-brain barrier in mice and humans and does not cause long-term neurologic damage (9). Furthermore, the clinical response to the 3F8 mAb was associated with induction of an idiotype network which included anti-anti-idiotypic (Ab3) and anti-GD2 (Ab3′) antibodies and prolonged survival in children with stage IV neuroblastoma (16, 17).

Currently, the GD2 lactone-keyhole limpet hemocyanin (KLH) conjugate vaccine shows promise for active, specific immunotherapy in patients with malignant melanoma (18). However, the potential difficulty associated with this immunization approach resides in the induction of relatively low levels of GD2-specific immunoglobulin G (IgG) antibody responses (18), raising the possibility that the GD2 conjugate may not be sufficiently immunogenic in immunosuppressed individuals (reviewed in ref. 19). It is also probable that the carrier protein, due to a highly cross-reactive nature and strong immunogenicity, can act as a polyclonal activator causing suppression of protective immune responses. For example, immunization of mice with a glycoconjugate vaccine composed of the glucuronoxylomannan (GXM) component of the cryptococcal capsular polysaccharide conjugated to tetanus toxoid produced antibodies that were both protective and nonprotective (20). Similarly, peptide mimetics of GXM did not elicit a strong immune response to GXM when they were conjugated to KLH. Rather, KLH contained carbohydrate antigens that elicited an anti-GXM response to nonprotective epitopes (20). Because nonprotective antibodies block the efficacy of protective humoral responses, an effective vaccination strategy must focus on the induction of antibody responses to a protective epitope (20–22).

In a search for a method of generating a vaccine to GD2 ganglioside that is T-cell dependent, highly immunogenic, and specifically directs the antibody response to a protective epitope, we have focused on the GD2 mimetic peptides as surrogate antigens. Mimetic peptides represent a very promising tool to overcome T-cell independence of some carbohydrate antigens (23) and offer an attractive alternative to glycoconjugates (18) or anti-idiotypic antibodies (24–26). The chemical composition and purity of synthesized peptides can be precisely defined, and immunogenicity significantly enhanced, by polymerization. Peptide synthesis may be more practical than synthesis of carbohydrate-protein conjugates or production of anti-idiotypes. Furthermore, mimetic

Requests for reprints: Danuta Kozbor, Department of Immunology, Roswell Park Cancer Institute, Elm and Carlton Streets, Buffalo, NY 14263. Phone: 215-355-4549; Fax: 716-845-8906; E-mail: danuta.kozbor@roswellpark.org.

peptides can also provide immunologic memory for a carbohydrate boost (27) and can be engineered into plasmids for DNA vaccination to increase the level and persistence of carbohydrate-specific immune responses (28).

In these studies, we investigated whether interconversion of GD2 ganglioside into a peptide mimetic form would induce GD2-specific IgG antibody responses by DNA vaccination in mice. Screening of the X_{15} phage display peptide library with GD2-specific 14G2a mAb, followed by molecular modeling and mutagenesis studies, led to identification of the GD2 mimetic peptide 47-LDA. Immunization of BALB/c mice with peptide 47-LDA–encoded plasmid DNA elicited GD2 cross-reactive IgG antibody responses, which were enhanced on subsequent boost with GD2 ganglioside. The vaccine-induced GD2-specific antibodies were capable of complement-dependent cytotoxicity and induced protection against s.c. growth of human GD2-positive MV3 melanoma cells in severe combined immunodeficient (SCID) mice. This information contributes to our understanding of the structural mimicry of antigenic determinants defined by 14G2a mAb on the GD2 mimetic peptide as well as the effectiveness of this vaccination approach in immunotherapy against GD2-positive tumor cells.

Materials and Methods

Animals and cell lines. BALB/c and SCID/NCr (BALB/c background) mice, 6 to 8 weeks of age, were purchased from the National Cancer Institute-Frederick Animal Production Program (Frederick, MD). The animals were housed under pathogen-free conditions in the Animal Facility at Roswell Park Cancer Institute, Buffalo, NY. GD2-positive human IMR-32 neuroblastoma (29) and HT-144 melanoma (30) cell lines, and GD2-negative human 293T fibroblasts (31) were obtained from the American Type Culture Collection (ATCC; Rockville, MD). The GD2-positive MV3 human melanoma cell line (32) was provided by Dr. G. van Muijen (University of Nijmegen, Nijmegen, the Netherlands). The hybridoma cell line secreting GD2-specific mAb 14G2a (IgG2a; ref. 33) was provided by Dr. Ralph A. Reisfeld (The Scripps Research Institute, La Jolla, CA), whereas 126 hybrid cell line secreting GD2-specific IgM mAb was obtained from ATCC.

Antibodies. The anti-GD2 mAb 14G2a was purified from culture supernatant by affinity chromatography on the HiTrap Protein G HP column (Amersham Pharmacia Biotech, Piscataway, NJ). Horseradish peroxidase (HRP)–conjugated anti-M13 mAb was purchased from Amersham Pharmacia Biotech. HRP- and alkaline phosphatase–conjugated goat anti-mouse IgG and IgM antibodies as well as HRP-conjugated rabbit anti-human Ig were purchased from Sigma (St. Louis, MO). FITC-conjugated $F(ab')_2$ fragment of goat anti-mouse Ig was purchased from ICN Biomedicals, Inc. (Costa Mesa, CA). The alkaline phosphatase–conjugated rat anti-mouse IgG1, IgG2a, IgG2b, or IgG3 antibodies were purchased from BD PharMingen (San Diego, CA).

Serum specimens from patients with neuroblastoma. Serum specimens were prepared from peripheral blood obtained from five patients who were diagnosed with neuroblastoma at Roswell Park Cancer Institute. Patients 12 and 41 had progressed and metastasized tumor at the time of blood sample collection. Patient 23 was diagnosed with stage IV neuroblastoma and remained in remission for many years after bone marrow transplantation. This patient was in relapse at the time of sample collection. Patients 35 and 50 were at stage I neuroblastoma and remained in remission for many years. Our investigation had prior approval of the Institutional Review Board on human experimentation.

Isolation of mimetic peptides from the X_{15} peptide library. The phage display peptide library X_{15} used for panning with 14G2a mAb was kindly provided by Dr. J.K. Scott (Simon Fraser University, Burnaby, British Columbia, Canada). The library displayed 15-amino-acid, random, linear peptide inserts at the N terminus of the synthetic pVIII major coat protein of bacteriophage vector f88.4 (34). Panning of the amplified peptide library X_{15} with 14G2a was done as described (35). The reactivity of random phage clones with 14G2a mAb was done by the immunoscreening assay as described (35). The nucleotide sequence of peptide inserts was determined by the dideoxynucleotide chain termination method (36) using the M13 primer (5′-AGTAGCAGAAGCCTGAAGA-3′) in the Biopolymer Facility at Roswell Park Cancer Institute.

Synthetic peptides. The amino acid sequence of the synthetic peptides isolated from the X_{15} phage display peptide library is shown in Table 1. All peptides were synthesized and characterized in the Molecular Genetics Instrumentation Facility at the University of Georgia (Athens, GA).

Molecular modeling. The computational part of this work consisted of several steps that included identification of the template structure for the generation of molecular model of the variable heavy (VH) and light (VL) immunoglobulin domains of 14.18 mAb, which is an isotype switch variant

Table 1. Characterization of phage clones identified by panning the X_{15} phage display library with mAb 14G2a

Phage clones	Frequency (%)*	Phage binding to 14G2a mAb ($A_{450\ nm}$)†	Peptide sequence‡	IC_{50} of peptide-mediated inhibition of 14G2a mAb binding to IMR-32 cells (μmol/L)§
9	3/22 (13.6)	0.415 ± 0.03	EANAPLDMGVFFEHN	16.2 ± 1.5
30	1/22 (4.5)	0.470 ± 0.04	NNNQLDCLLFVRQCK	112.0 ± 21.0
47	9/22 (40.9)	0.452 ± 0.04	EDPSHSLGLDVALFM	5.0 ± 0.4
51	7/22 (31.8)	0.408 ± 0.01	QTPETLTLFPPNWMN	15.4 ± 2.2
54	1/22 (4.5)	0.335 ± 0.06	RLTSPADMGSFLFNL	227.0 ± 18.0
56	1/22 (4.5)	0.396 ± 0.03	RTTLGHHLDFTLWTA	60.0 ± 5.4

*Twenty-two phage clones isolated from the X_{15} phage display peptide library were divided into six families based on the DNA sequence analysis.
† For reverse ELISA, 14G2a mAb-coated wells were incubated with positive phage clones (0.5×10^{12} transforming units), washed and incubated with HRP-conjugated anti-M13 mAb. After a final wash, the reaction was developed with the HRP substrate and quantified by reading the absorbance at 450 nm in a plate reader. The wells incubated with negative clones remained nearly colorless.
‡ The amino acid sequence of the peptides was determined from the nucleotide sequence of 14G2a mAb-isolated phage clones.
§ Dose-dependent inhibition of the 14G2a antibody binding to GD2-positive IMR-32 cells by synthetic peptides isolated from the X_{15} phage display peptide library. Varying amounts of the competitors were incubated overnight with 14G2a antibody (1 μg/mL) at 4°C. The mixtures were transferred to IMR-32 cells, and the inhibition of 14G2a binding to cellular GD2 was measured after staining with FITC-conjugated secondary antibody by flow cytometry analysis.

of 14G2a (33). The amino acid sequence of the VL κ-chain (amino acids 1-113: DVVMTQTPLSLPVSLGDQASISCRSSQSLVHRNGNTYLHWYLQKPGQSPKLLIHKVSNRFSGVPDRFSGSGSGTDFTLKISRVEAEDLGVYFCSQSTHVPPLTFGAGTKLELK) and the VH chain (amino acids 114-228: EVQLLQSGPELEKPSASVMISCKASGSSFTGYNMNWVRQNIGKSLEWIGAIDPYYGGTSYNQKFKGRATLTVDKSSSTAYMHLKSLTSEDSVYYCVSGMEYWGQGTSVTVSS) was provided by Dr. Stephen Gillies (EMD Pharmaceuticals, Billerica, MA). The template structure of the VH and VL domains was identified by the PSI-BLAST program (37) using the PDB code 1jp5 (38, 39). After three PSI-BLAST iterations, a sequence-to-structure alignment of the model sequence and template structure was generated. The alignment was subsequently used in the antibody model building with an automated molecular modeling program, MODELLER v.6.2 (40). The resulting model was refined by the molecular minimization procedure that employed the AMBER force field (41). Then, an initial structure of the peptide was built using the Biodesigner molecular modeling program (http://www.pirx.com/biodesigner/index.shtml). Subsequently, the structure of the peptide was oriented by hand close to the putative antibody-combining site (using the Biodesigner program) and the entire system was modeled using a lattice Monte Carlo simulation algorithm (42). The lowest energy conformation was selected as a final model with three united atoms per residue that corresponded to the α carbon, β carbon, and the center of the remaining portion of the side chain (where applicable). These united atoms were the centers of interactions in the model force field, which consisted of a set of knowledge based potentials derived from a statistical analysis of structural regularities seen in proteins and polypeptides (37). The CABS (CA-β carbon-Side group) molecular modeling tool (37) was employed, and the full-atom model reconstruction step was carried out using PULCHRA (43). The final molecular model of the 14G2a V region and the peptide was refined using the AMBER force field.

Alanine-scanning mutagenesis. Individual substitution of amino acids in the GD2 mimetic peptide 47 with Ala was carried out by a site-directed mutagenesis using the phage clone 47 with specific oligonucleotide primers and a reagent kit from Stratagene (La Jolla, Ca) according to the protocol of the manufacturer.

Construction of the 47-LDA expression vector. The human codon-optimized oligonucleotide, corresponding to the GD2 mimetic peptide 47-LDA (EDPSHSLGLDAALFM) and two universal T helper (Th) peptides PADRE (AKFVAAWTLKAAA; ref. 44) and $P18_{MN}$ (CKRKIHIGPGQAFYT; ref. 45), was generated using four 60-mer primers with 15-nucleotide overlaps by a PCR amplification method. Oligonucleotides corresponding to the spacer sequence KCKRQC and the Th epitopes were inserted upstream of the 47-LDA peptide sequence. To avoid the generation of junctional epitopes, an oligonucleotide linker corresponding to the GPGPG sequence was inserted between PADRE, $P18_{MN}$, and 47-LDA. The entire 47-LDA construct was synthesized with upstream (5′-AAAGCGGCCGCCAAGTGCAAGCGCCAG-3′) and downstream (5′-GCCGGGGATCCCTCAGCCCTTAGGCAT-3′) primers containing the *Not*I and *Bam*HI restriction enzyme cleavage sequences, respectively. The final PCR product was purified and cloned into *Not*I and *Bam*HI sites of the pNGVL-7 vector (University of Michigan, Ann Arbor, MI) by fusing the 47-LDA polytope open reading frame with tissue plasminogen activator secretory signal sequence (tPA) under the control of human cytomegalovirus immediate early promoter.

Flow cytometry analysis and immunoblotting. Transient transfection of 293 T cells was done with the 47-LDA construct or sham vector using Lipofectamine Reagent (Invitrogen, Carlsbad, CA) according to the protocol of the manufacturer. The intracellular staining of the transfected cells was carried out using 14G2a mAb and BD Cytofix/Cytoperm kit (PharMingen) according to the protocol of the manufacturer. Culture supernatants from the transfected cells were concentrated 10-fold on Centriplus YM-3 filters (Amicon, Bedford, MA), separated by SDS-12% PAGE, and analyzed by immunoblotting with 14G2a mAb using enhanced chemiluminescence Western blotting detection reagent (Amersham Pharmacia Biotech) according to the protocol of the manufacturer.

Immunization. Six-week-old BALB/c mice ($n = 5$ per group) were injected i.m. in the quadriceps with 100 μg of plasmid encoding the 47-LDA construct or sham vector on days 0, 21, and 42. For the GD2 boost, the minigene- or sham vector–immunized mice were injected i.p. with 40 μg of GD2 (Voigt Global Distribution LLC, Kansas City, MO) emulsified in incomplete Freund's adjuvant (Sigma) 3 weeks after DNA immunization. Sera were collected 3 weeks after the last immunization and analyzed for GD2-specific antibody responses.

Measurements of anti-GD2 antibody titers and isotypes. The level of GD2 cross-reactive antibodies was determined by testing serial 3-fold dilutions of sera from the immunized mice by ELISA with GD2-coated wells as described elsewhere (46). Subisotyping of serum IgG antibody responses was carried out with alkaline phosphatase–conjugated rat anti-mouse IgG1, IgG2a, IgG2b, or IgG3 secondary antibodies (BD PharMingen). Sample dilutions were considered positive if the absorbance recorded for that dilution was significantly different from the absorbance recorded for the control sera from mice immunized with the sham vector using paired Student's t test ($P < 0.05$). As positive controls, GD2-specific 126 (IgM) and 14G2a (IgG2a) mAbs were included in the assay. The vaccine-induced GD2 cross-reactive IgG antibody responses were quantified from a standard curve generated concurrently using GD2-specific 14G2a mAb.

Antibody inhibition assays. For the inhibition assay, varying amounts of synthetic peptides or soluble GD2 ganglioside were mixed with 14G2a mAb or the vaccine-induced antibodies used at a concentration of 1 μg/mL. Following an overnight incubation at 4°C, the mixtures were added to IMR-32 cells and the inhibition was determined by immunofluorescence staining and flow cytometry analysis. In some experiments, ELISA assay was used to determine the ability of soluble GD2 ganglioside to inhibit the antibody binding to GD2-coated wells.

Complement-dependent cytotoxicity assay. The complement-mediated lysis of tumor cells was assayed at serum dilutions of 1:30 and 1:100 with ^{51}Cr-labeled IMR-32 and HT-144 cells, and the rabbit complement (Cedarlane Laboratories, Ltd., Hornby, Ontario, Canada) as previously described (47). The percent of specific lysis was calculated as [(cpm experimental release − cpm spontaneous release) / (cpm maximum release − cpm spontaneous release)] × 100.

The severe combined immunodeficient mouse xenograft tumor challenge and antitumor therapy. Groups of five female SCID mice were injected s.c. in the lateral flank with 10^6 human MV3 melanoma cells. Tumor growth was monitored by measuring s.c. tumors once to thrice a week with a microcaliper and determining tumor volume (width × length × width / 2 = mm^3). Mice injected with the s.c. tumors were treated, beginning on day 3 after tumor challenge, for 7 consecutive days with 5 μg of GD2 cross-reactive antibody per day (7 days × 5 μg/d) by 100-μL tail vein injections. Then, the antibodies were administered every 3 days for a 2-week period. In parallel, control mice that were inoculated with MV3 tumor were treated with 5 μg/d of murine IgG. The GD2-specific antibodies were purified from pooled sera of 47-LDA minigene– and GD2-immunized BALB/c mice using the HiTrap Protein G HP column (Amersham Pharmacia Biotech) according to the protocol of the manufacturer. The concentration of GD2-specific IgG antibodies was quantified by GD2-specific ELISA from a standard curve generated concurrently using GD2-reactive 14G2a mAb.

Statistical analysis. The statistical significance of the difference between groups presented in Figs. 1 and 4*A* was done using a two-tailed Student's t test assuming equal variance. In Table 2, mixed model ANOVAs (48) were used to compare mean values of GD2-specific antibody responses between mice immunized with the 47-LDA minigene or sham vector vaccine alone or in combination with GD2 booster immunization. In Fig. 4*B* and *C*, the P values for the pairwise group comparisons for the average tumor growth over days 20 to 46 were computed using the nonparametric Wilcoxon's rank-sum test. Data were presented as arithmetic mean ± SD and analyzed using the JMP program (SAS Institute, Inc., Cary, NC) on a Windows-based platform.

Results

Characterization of peptides isolated from the X_{15} phage display peptide library with 14G2a monoclonal antibody. Fifty-six phage clones isolated at the end of the fourth round of screening the X_{15} phage display peptide library with anti-GD2 mAb 14G2a were

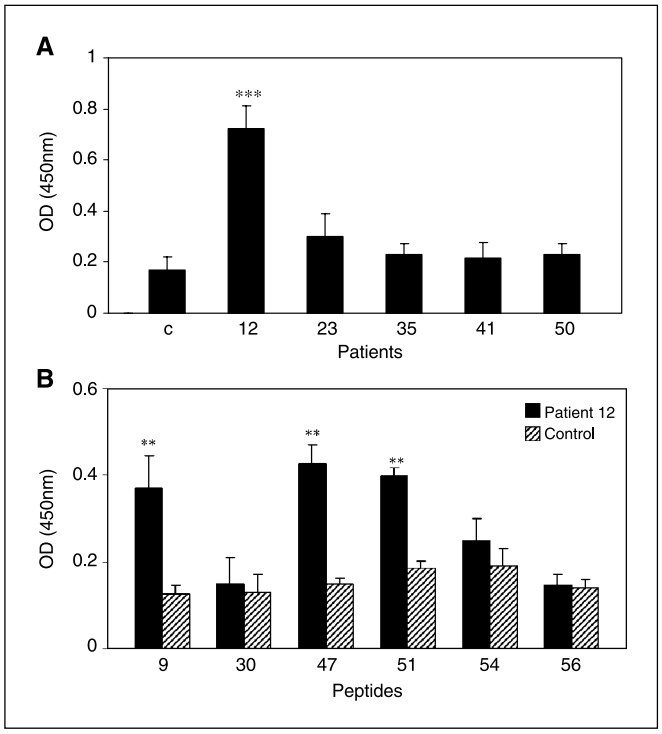

Figure 1. The reactivity of sera from neuroblastoma-bearing patients with GD2 ganglioside (*A*) and GD2 mimetic peptides (*B*). Sera from five patients with neuroblastoma and from a healthy individual (c) were tested for the presence of GD2-specific antibody by ELISA using HRP-conjugated anti-human polyvalent Ig (*A*). Sera from patient 12 with detectable GD2-specific reactivity (*black columns*) and from a healthy donor (*hatched columns*) were analyzed for binding to peptides 9, 30, 47, 51, 54, and 56 by ELISA (*B*). *Columns,* mean of triplicate determinations of 1:10 serum dilution, expressed as absorbance at 405 nm; *bars,* SD. ***, $P < 0.0001$ and **, $P < 0.001$ compared with serum specimens from a healthy donor using Student's *t* test.

tested by immunoblotting and reverse ELISA to confirm their reactivity with 14G2a. Twenty-two clones that were identified as positive by these two methods fell into six phage families based on the DNA sequence analysis (Table 1). Families 9, 47, and 51 were represented by several repetitive phage clones, whereas families 30, 54, and 56 consisted only of one member. To establish structural similarities of the isolates clones with GD2 ganglioside, synthetic peptides representing the individual phage families were analyzed for the ability to inhibit the binding of 14G2a mAb to GD2-positive IMR-32 neuroblastoma cells. As shown in Table 1, the highest level of inhibition of 14G2a antibody binding was achieved with peptide 47 (IC_{50} of 5.0 ± 0.4 μmol/L). For peptides 9 and 51, the respective IC_{50} values were 16.2 ± 1.5 and 15.4 ± 2.2 μmol/L, whereas peptides 56, 30, and 54 had low inhibitory activities with IC_{50} values ranging from 60 to 227 μmol/L.

Recognition of the GD2 mimetic peptides by anti-GD2 serum antibodies from patients with neuroblastoma. To further characterize similarity between the isolated peptides and GD2 ganglioside, we examined their reactivity with GD2-specific antibodies in sera from neuroblastoma-bearing patients. Because GD2-specific antibody responses occur in less than 20% of patients with GD2-positive tumors (49), GD2-specific ELISA was first used to identify the ganglioside-reactive sera. As shown in Fig. 1*A*, only one of five patients (patient 12) analyzed exhibited GD2-specific antibodies detectable at the serum dilution of 1:10. Subsequently, serum specimens from patient 12 were used to investigate reactivity with the isolated GD2 mimetic peptides in ELISA. Figure 1*B* shows that at the serum dilution of 1:10, a specific binding was measured with peptides 47, 9, and 51 ($P < 0.001$). Other peptides showed reactivity comparable to that obtained with the control serum of a healthy individual.

Molecular modeling of the GD2 mimetic peptide interaction with the antibody-combining site of 14G2a. To understand the structural basis for antigenicity of the GD2 mimetic peptides, we analyzed a three-dimensional structure of peptide 47 complexed with the VH_{14G2a} and VL_{14G2a} chains of 14G2a mAb. This peptide was selected for the study because it was the most effective in inhibiting the binding of 14G2a to cellular GD2 and reacts with GD2-specific antibodies from the neuroblastoma-bearing patient. Peptide 47 also blocked the binding of peptides 9 and 51 to 14G2a mAb (not shown), suggesting that these three peptides mimic an overlapping epitope of GD2.

Table 2. Anti-GD2 antibody responses in sera of mice immunized by the prime-boost strategy with the 47-LDA construct and GD2

Immunization*		Titer of GD2 cross-reactive antibodies†		Mean fluorescence intensity of serum binding to GD2-positive cells‡	
Construct	GD2 ganglioside	IgM	IgG	IMR-32	HT-144
Sham	−	NA§	NA	7.4 ± 1.8	6.5 ± 1.4
Sham	+	178 ± 45	32 ± 9	28.5 ± 6.5	31.6 ± 4.9
47-LDA	−	63 ± 12	910 ± 33	47.9 ± 5.3	54.4 ± 6.6
47-LDA	+	152 ± 33	1,820 ± 250	86.4 ± 8.7	78.8 ± 5.9

*BALB/c mice ($n = 5$) were immunized by the 47-LDA construct or sham plasmid alone or in a combination with GD2 boost. Blood was collected 3 weeks after the last immunization and analyzed for the presence of GD2 cross-reactive antibody responses.

† The titers of GD2 cross-reactive IgM and IgG antibodies were determined by ELISA as described in Materials and Methods. The titers are shown as the highest serum dilutions with significantly different OD as compared with sera from vector-immunized mice using paired Student's *t* test ($P < 0.05$).

‡ The binding of sera (dilution 1:50) from mice immunized by the DNA vaccine alone or in combination with GD2 boost to GD2-positive IMR-32 neuroblastoma and HT-144 melanoma cells was analyzed using FITC-conjugated secondary antibody. Cells were analyzed by flow cytometry on FACScan. Results are presented as mean fluorescence intensity and presented as mean values ± SD of four independent experiments.

§NA, not applicable.

The interaction of peptide 47 with the antibody-combining site of 14G2a was analyzed by the refined lowest energy molecular model using the lattice Monte Carlo simulation algorithm and the AMBER force field. This approach positioned the peptide fragment within the antibody-combining site free of steric conflicts. As shown in Fig. 2*A*, the computer-screening search identified 23 residues in the VH_{14G2a} and VL_{14G2a} chains that interacted with peptide 47. Some of them, such as His-31 of the κ chain and Met-213 of the VH_{14G2a} chain, contacted three and four residues of the peptide, respectively. The residues within the VH_{14G2a} and VL_{14G2a} chains that seemed to be important for the positioning peptide 47 in the antibody-combining site included Met-213 of the VH_{14G2a} chain interacting with Asp-2, Pro-3, Ser-6, and Leu-7 as well as His-31 of the VL_{14G2a} chain interacting with Leu-9, Asp-10, and Leu-13. Other residues, such as Asn-33, Tyr-37, Ser-96, Arg-32, Val-99, Thr-97, and Pro-101 of the VL_{14G2a} region, contacted two or three different amino acids within the peptide motif from Leu-7 to Met-15 (LGLDVALFM). Among these amino acids, Leu-7 interacted with four residues of the VL_{14G2a} chain and with two residues in VH_{14G2a} domain (Fig. 2*A* and *B*). Other residues of the peptide from Leu-9 to Phe-14 interacted solely with amino acids located in the VL_{14G2a} chain. The C-terminal Met-15 anchored the end of the peptide in a pocket formed by Val-99 and Pro-101 in the VL_{14G2a} chain, and Ser-172 in the VH_{14G2a} segment. On the other hand, the interaction of residues from Glu-1 to Ser-6 in the N-terminal part of the peptide was flexible and limited to a contact with one or two amino acids within the VL_{14G2a} or VH_{14G2a} chain.

Consistent with the observed flexibility of the N-terminal region of peptide 47 from Glu-1 to Ser-6, replacement of individual residues within this segment with Ala had less than 10% effect on the binding to 14G2a. Thus, based on the structure-based computer mapping and Ala-scanning technique, we identified the LGLDVALFM sequence stretch in peptide 47 as essential for interacting with the antibody-combining site of 14G2a (Fig. 2*B*). Replacement of Val within this segment with Ala revealed that peptide 47-LDA was at least 2-fold more effective than the parental peptide 47 in inhibiting 14G2a antibody binding to IMR-32 cells

A

Peptide 47	VL_{14G2a}	VH_{14G2a}
Glu-1	-	Asp-165, Pro-166
Asp-2	-	Met-213
Pro-3	-	Tyr-145, Met-213
Ser-4	-	Glu-214
His-5	Asn-33, Lys-55	-
Ser-6	His-54	Met-213, Glu-214
Leu-7	Tyr-37, His-39, Lys-55, Ser-96	Gly-212, Met-213
Gly-8	-	-
Leu-9	His-31, Asn-33, Tyr-37	-
Asp-10	His-31	-
Val-11	Arg-32, Asn-33	-
Ala-12	Val-99	-
Leu-13	His-31, Arg-32, Thr-97, His-98, Pro-101	-
Phe-14	Ser-96, Thr-97, Val-99, Pro-101	-
Met-15	Val-99, Pro-101	Ser-172

B

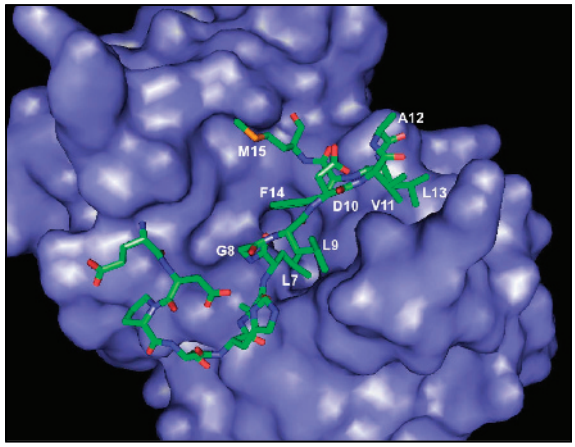

Figure 2. Hydrogen bond contact between residues of peptide 47 and the VL and VH chains of 14G2a mAb, and the molecular model of the three-dimensional structure of peptide 47 complexed with the 14G2a antibody–combining site. *A,* amino acid sequence of VH_{14G2a} and VL_{14G2a} chains was used to create a template for the generation of appropriate sequence-to-structure alignments between the mimicking peptide and the antibody-combining site as described in Materials and Methods. The contacts between the amino acids of peptide 47 and the V region of 14G2a antibody occur when a distance between any pair of the heavy atoms is shorter than 4.5 Å. The symbol (–) denotes lack of interaction between peptide 47 and the V region of 14G2a mAb. *B,* atoms are depicted by colors: *green*, carbon; *red*, oxygen; *blue*, nitrogen; *orange*, sulfur; hydrogens are not shown. *Light blue,* solvent accessibility surface of the receptor protein.

(IC_{50} of 2.4 ± 0.3 versus 5.0 ± 0.4 μmol/L) as determined by immunofluorescence staining and flow cytometry analysis (not shown). The AMBER force field energy of the 14G2a antibody and the mutated peptide 47-LDA complex was also lower than that formed with peptide 47 (−55.6 versus −47.9 kcal/mol), suggesting an energetic gain by the Ala substitution. On the other hand, replacement of other residues within the LGLDVALFM sequence stretch either abolished (residues Lys and Asp) or reduced by over 40% (residues Lys, Gly, Lys, Phe, and Met) the binding of the mutated peptides to 14G2a mAb.

Generation of the 47-LDA minigene vaccine. To investigate whether the identified GD2 mimetic peptide would induce GD2 cross-reactive IgG antibody responses, we generated a codon-optimized 47-LDA construct expressing the chimeric peptide consisting of the tPA leader sequence fused in-frame with the Th peptides PADRE and $P18_{MN}$ inserted upstream of the mimetic peptide 47-LDA. It was rationalized that the leader sequence would allow exogenous expression of the 47-LDA peptide, whereas the PADRE and $P18_{MN}$ epitopes would facilitate binding of the 47-LDA polytope to multiple, nonoverlapping MHC class II molecules of both mice and humans (46, 47).

Direct sequencing of the 47-LDA construct confirmed the presence of an uncorrupted open reading frame encoding the tPA leader sequence together with PADRE, $P18_{MN}$, and 47-LDA peptides. The immunofluorescence staining of 47-LDA–transfected 293 T cells with 14G2a mAb followed by flow cytometry analysis was done 48 hours after transfection to determine the intracellular expression of the 47-LDA polytope. Figure 3*A* revealed a high level of 47-LDA polytope expression compared with that in cells transfected with the sham vector (Fig. 3*B*). The secretion of the chimeric peptide into culture supernatant from 47-LDA transfectants was confirmed by immunoblotting with 14G2a mAb. As shown in Fig. 3*C*, a prominent band of 6.6 kDa was detected with 14G2a mAb in culture supernatants harvested from 47-LDA transfectants. No band was present in supernatants prepared from cells transfected with the sham plasmid. Altogether, these results showed that the GD2 mimetic peptide expressed in the 47-LDA minigene retained native antigenic determinants of the synthetic peptide recognized by 14G2a mAb.

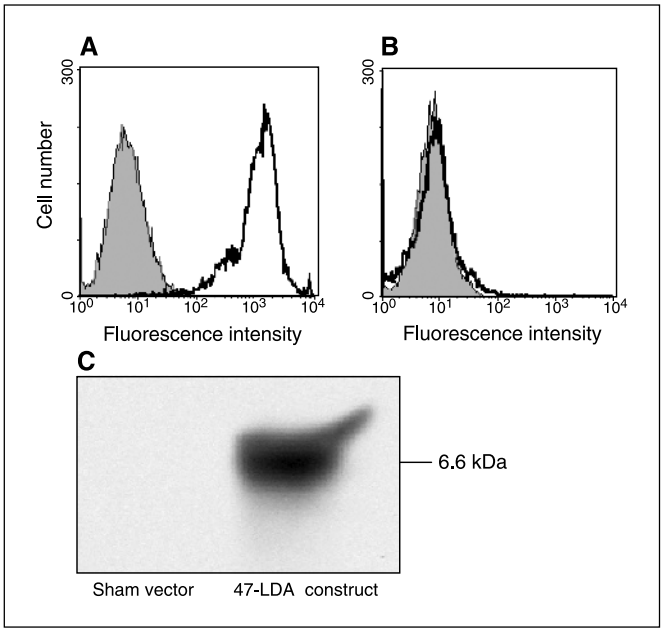

Figure 3. Flow cytometry and immunoblotting analyses of 47-LDA polypeptide expression in 293 T-cell transfectants. 293 T fibroblasts were transfected with the 47-LDA construct encoding PADRE, Env, and 47-LDA epitopes (*A*) or with the sham vector (*B*). The transgene expression was analyzed 48 hours after transfection by intracellular staining with 14G2a mAb followed by the FITC-conjugated $F(ab)_2$ portion of goat anti-mouse Ig. Cells were analyzed by flow cytometry on FACScan. *Light gray area,* transfectants stained with the secondary antibody only. *C,* culture supernatants from 293 T cells transfected with the sham vector or 47-LDA construct were separated by SDS-PAGE and analyzed by immunoblotting with 14G2a mAb.

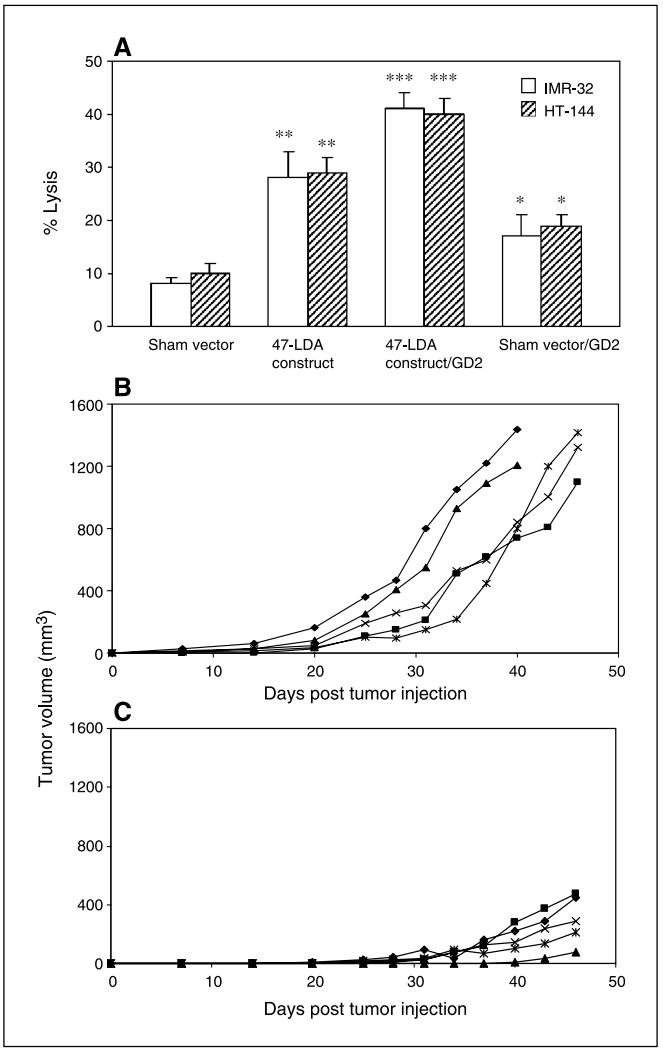

Figure 4. Protective efficacy of the vaccine-induced GD2-specific antibodies against GD2-positive tumor cells *in vitro* and *in vivo*. *A,* complement-dependent cytotoxicity assay with human GD2-positive IMR-32 neuroblastoma and HT-144 melanoma cells and sera from BALB/c mice immunized with the 47-LDA minigene or sham vector alone or in combination with the GD2 ganglioside boost. Complement-dependent cytotoxicity experiments were done at 1:30 serum dilution. *Open* and *hatched columns,* IMR-32 and HT-144 cells, respectively. *Columns,* mean of experiments including four mice per group; *bars,* SD. ***, $P < 0.0001$; **, $P < 0.005$; *, $P < 0.05$ compared with sera from sham vector–immunized animals using Student's *t* test. *B,* efficacy of the vaccine-induced GD2 cross-reactive antibodies against s.c. growth of human MV3 melanoma cells in SCID mice. Groups of five mice were treated i.v. with 5 μg/d of mouse IgG (*A*) or GD2-specific IgG antibodies (*B*) beginning on day 3 after s.c. injection of 10^6 MV3 tumor cells as described in Materials and Methods. Animals were examined daily until the tumor became palpable, after which tumor growth was monitored by measuring s.c. tumors once to thrice a week. *Lines,* tumor growth in individual mice.

Vaccination with the 47-LDA construct induces GD2 cross-reactive antibody responses. An ELISA assay was used to analyze the level of antibody responses to GD2 ganglioside in sera of BALB/c mice immunized by three i.m. injections with the 47-LDA construct or sham vector. In some experiments, 47-LDA– or sham vector–immunized mice were boosted with GD2 ganglioside based on previous studies which showed that the immunization with plasmid DNA followed by a carbohydrate boost induces higher levels of immune responses compared with those elicited by each of these strategies alone (28). Results with 3-fold diluted sera showed statistically significant differences in the levels of GD2 cross-reactive IgG antibody responses among the immunized groups of mice ($P < 0.0001$; Table 2). In contrast, the induction of GD2 cross-reactive IgM antibody responses by the 47-LDA minigene construct or GD2 ganglioside was low and did not differ significantly among the immunized animals. The end-point titer of GD2 cross-reactive IgG antibody responses in 47-LDA minigene–immunized mice was ~30-fold higher than that induced by priming with the sham vector and GD2 ganglioside boost ($P = 0.009$). Furthermore, the booster immunization with GD2 of the minigene-primed mice elicited over 2-fold increases in titers of GD2 cross-reactive IgG antibody responses ($P = 0.03$; Table 2), suggesting that priming with the 47-LDA construct generated GD2 cross-reactive antibody responses that were further expanded by a booster immunization with the nominal antigen. Subisotyping of GD2-specific IgG antibodies in animals immunized by the prime-boost strategy revealed comparable levels of IgG2a and IgG1 with the respective titers of 1:560 and 1:410 (not shown), whereas GD2-specific IgG2b and IgG3 antibody responses were at background levels.

The specificity of the vaccine-induced antibody responses to GD2 was confirmed in the inhibition assay, which showed that the binding of 1 μg/mL of serum IgG to GD2-coated wells was inhibited by soluble GD2 ganglioside with IC_{50} of 18.2 ± 0.5 μmol/L. These results, together with those which showed that sera from mice immunized with a construct expressing only PADRE and $P18_{MN}$ peptides did not induce measurable anti-GD2 antibodies, indicate that the GD2-specific humoral responses in 47-LDA–immunized mice were induced solely by the GD2 mimetic peptide.

Vaccine-induced antibodies recognize cell surface–associated GD2 ganglioside. We next investigated whether antibodies induced by the minigene vaccine alone or in combination with the GD2 boost were capable of recognizing GD2 ganglioside expressed on the surface of tumor cells. For these experiments, IMR-32 and HT-144 cells were incubated under a saturated condition (dilution 1:50) with sera from the immunized mice followed by staining with FITC-conjugated secondary antibodies and flow cytometry analysis. As shown in Table 2, the mean fluorescence intensities of GD2-positive IMR-32 and HT-144 cells incubated with sera from 47-LDA–immunized mice were ~10-fold higher than those detected with sera from the sham vector–immunized animals ($P < 0.0001$). The latter group of mice exhibited some reactivity with IMR-32 and HT-144 cells after the GD2 booster immunization although the mean fluorescence intensity was lower than that obtained after 47-LDA minigene vaccine ($P < 0.03$). Consistent with the ELISA assay, the antibody responses induced by the prime-boost strategy with the 47-LDA construct and GD2 ganglioside exhibited over 2-fold increases in the reactivity with IMR-32 and HT-144 cells compared with those elicited by the 47-LDA vaccine. The specificity of the binding was further confirmed by inhibition assay, which showed that the reactivity of 1 μg/mL of vaccine-induced IgG antibody with IMR-32 cells was inhibited by soluble GD2 ganglioside with an estimated IC_{50} of 2.4 ± 0.3 μmol/L.

Cytolytic activity of the minigene-induced antibodies against GD2-positive tumor cells. The functional properties of serum antibodies induced by the 47-LDA construct alone or in combination with the GD2 booster immunization were tested in complement-dependent lysis of IMR-32 and HT-144 cells using a standard ^{51}Cr release assay. Figure 4*A* shows that at dilution 1:30, sera from mice immunized with the 47-LDA construct induced ~27% specific lysis of the target cells, which was significantly higher compared with less than 10% lysis mediated by sera from the control mice ($P < 0.005$). The booster immunization of control mice with GD2 increased the cytolytic activity of the sera against both targets ($P < 0.05$), presumably due to the induction of GD2 cross-reactive IgM antibody responses by the ganglioside vaccine. The highest level of specific lysis against IMR-32 and HT-144 cells was obtained in 47-LDA–immunized mice after the booster immunization with GD2, which was ~5-fold increased compared with the control group ($P < 0.0001$). Sera from mice immunized by the 47-LDA minigene and GD2 prime-boost strategy mediated over 40% specific lysis against the GD2-expressing tumor cells, and the activity remained at a detectable level at the serum dilution of 1:100 (not shown).

Tumor regression of GD2 ganglioside–expressing human MV3 melanoma cells in severe combined immunodeficient mice after systemic anti-GD2 antibody therapy. The therapeutic efficacy of GD2 cross-reactive IgG antibodies induced in mice by the prime-boost immunization with the 47-LDA minigene and GD2 ganglioside was assessed in the s.c. human MV3 melanoma model in SCID mice. The treatment regimen was based on that established for passive immunotherapy with the hu14.18-IL-2 immunocytokine fusion protein against s.c. growth of GD2-positive murine tumor cells in syngeneic mice (50, 51), and included administration of GD2-specific or control antibodies beginning on day 3 after tumor inoculation. As shown in Fig. 4*B*, all mice in the control group developed palpable tumors ~20 days after the challenge. Two of five mice exhibited progressive tumor growth and were sacrificed by day 40 after tumor inoculation. The three remaining tumor-bearing mice were sacrificed by day 46. In contrast, none of the SCID mice treated with GD2-specific antibody therapy exhibited tumor growth on day 20 (Fig. 4*C*). Three of five mice receiving the GD2 cross-reactive antibodies developed palpable tumors by day 25, and by day 40 only one mouse remained tumor free. All of the antibody-treated animals developed progressive tumors with time. However, the GD2-specific antibody therapy significantly reduced the mean rate of tumor growth compared with the control group as measured on day 25 (9.6 ± 10.2 versus 202 ± 107.5 mm^3; $P < 0.008$) and day 40 (150 ± 106.4 versus 1,006 ± 304.4 mm^3; $P < 0.009$). Thus, although mice did not show complete tumor resolution following the therapy with GD2-specific antibody in these particular experiments, likely reflecting the influence of MV3 tumor growth variability from experiment to experiment, there was a significant ($P < 0.0001$) decrease in tumor growth in the treated mice compared with the control group.

Discussion

The breaking of peripheral T-cell tolerance toward poorly immunogenic self-antigens expressed by tumor cells and the subsequent establishment of an effective tumor-protective immune response remain a major challenge for cancer immunotherapy.

Here, we showed for the first time that the GD2 mimetic peptide 47-LDA constructed into plasmid DNA was capable of inducing GD2 cross-reactive IgG antibody responses in mice. As GD2 ganglioside is highly expressed on brain and other tissues of neuroectodermal origin in both mice and humans (52–54), the induction of GD2 cross-reactive IgG antibody responses by the mimetic vaccine had to overcome immunologic tolerance in the immunized mice. Furthermore, the ability of the GD2 mimetic construct to induce GD2 cross-reactive humoral responses despite the intrinsic inability of BALB/c mice to generate a high titer of antibodies to ganglio-series ganglioside (55) raises the possibility that the immunization regimen employed in this study may prove effective in cancer-bearing patients. This, together with the finding of rapid activation of the minigene vaccine–induced GD2-specific IgG antibody responses on subsequent administration of GD2, suggests that priming with the GD2 mimotope followed by a booster with the nominal antigen would allow for the establishment of GD2-specific memory cells.

The ability of the mimetic peptide to mediate GD2 cross-reactive IgG antibody responses, which could not be effectively obtained by immunization with the GD2 ganglioside vaccine, stresses the importance of peptide mimetic vaccines in cancer-bearing patients. However, to the best of our knowledge, the structural basis of the GD2 glycolipid mimicry by the isolated peptides has never been explored in the experimental setting. Such analysis would require the establishment of molecular and structural interactions between the GD2 mimetic peptide and the antibody-combining site of 14G2a antibody. In fact, the LGLDVALFM sequence stretch of peptide 47 was shown by the refined lowest energy molecular model to be essential for this interaction, suggesting that the 14G2a antibody identified this core structure as the mimic of a particular GD2 configuration. However, recognition of this structure by the GD2-specific antibody could also rely on a sequence-dependent determinant present within and around the specific sequence motif. For example, replacement of the LD residues with Ala in the LGLDVALFM sequence stretch of peptide 47 completely abolished its binding to 14G2a antibody, whereas the same mutations had a smaller effect on the binding ability of mimetic peptides 9 and 51. Further analyses of the three-dimensional structure of 14G2a in complex with additional GD2 mimetic peptides may help to establish whether this or a similar mechanism underlies the reactivity of the antibody with multiple peptide conformations, and facilitate structure-based design of alternative peptides for the use as vaccines in cancer-bearing patients.

Identification of methods for inducing strong antibody responses to GD2 ganglioside would provide means for stimulating progress toward an effective vaccine against GD2-bearing tumors. As cancer vaccines that elicit primarily long-lasting antibody responses will likely be most effective in the minimal residual disease setting, the stage when tumor cells are few and dispersed, the induction of GD2-specific antibodies by the designed peptide mimetics alone or in the prime-boost combination with GD2 ganglioside may be beneficial for the tumor-bearing host. An additional support for this observation comes from the ability of GD2-specific antibodies in serum specimens from a patient with neuroblastoma to recognize the most antigenic peptides. The latter finding suggests that the mimetic peptide bearing an internal image of the GD2 ganglioside expressed on tumor cells *in vivo* may be capable of inducing GD2-specific immune responses in cancer patients. This condition remains essential for a candidate GD2 mimetic peptide to fulfill its promise as an alternative vaccine against GD2-expressing tumor cells (27).

It is clearly a unique property of this heterologous prime-boost immunization regimen using the minigene vaccine plus GD2 ganglioside to induce GD2 cross-reactive antibody responses that exhibited protection against s.c. GD2-positive tumor growth in the SCID mouse xenograft model. The protective efficacy of this approach may be further enhanced along with the administration of cytokines or other costimulatory molecules. For example, previous studies have shown that a constant infusion of interleukin 2 augmented the antitumor response induced by the hu14.18-IL-2 immunocytokine in mice with experimentally induced hepatic metastases and in animals bearing localized s.c. tumors (50). The combined treatment induced prolonged tumor eradication in most animals bearing s.c. tumors and involved both natural killer cells and T cells. These findings also suggest that engineering the mimotope into a hybrid plasmid, which can also include cytotoxic T-lymphocyte epitopes from a tumor target itself, would be expected to build an effector response that could decisively improve the tumor-protective immunity evoked by the minigene vaccine. Altogether, it is anticipated that results of our studies can lead to a rational design of therapeutic vaccines that may ultimately prove effective in clinical application against GD2-expressing tumor cells.

Acknowledgments

Received 6/25/2004; revised 12/17/2004; accepted 2/8/2005.

Grant support: Roswell Park Alliance Foundation (D. Kozbor) and the Ministry of Scientific Research and Information Technology 3P05A 00124 (H. Rokita).

The costs of publication of this article were defrayed in part by the payment of page charges. This article must therefore be hereby marked *advertisement* in accordance with 18 U.S.C. Section 1734 solely to indicate this fact.

We thank Drs. Ralph A. Reisfeld and Stephen Gillies for the reagents, Sandra Cieslak for help in blood sample collection, Earl Timm for help with flow cytometry analysis, and Michelle Detwiler for DNA sequencing.

References

1. Zhang S, Cordon-Cardo C, Zhang HS, et al. Selection of tumor antigens as targets for immune attack using immunohistochemistry: I. Focus on gangliosides. Int J Cancer 1997;73:42–9.
2. Reisfeld RA, Cheresh DA. Human tumor antigens. Adv Immunol 1987;40:323–77.
3. Cheresh DA, Varki AP, Varki NM, et al. A monoclonal antibody recognizes an *O*-acylated sialic acid in a human melanoma-associated ganglioside. J Biol Chem 1984;259:7453–9.
4. Schulz G, Cheresh DA, Varki NM, et al. Detection of ganglioside GD2 in tumor tissues and sera of neuroblastoma patients. Cancer Res 1984;44:5914–20.
5. Kramer K, Gerald WL, Kushner BH, et al. Disialoganglioside G(D2) loss following monoclonal antibody therapy is rare in neuroblastoma. Clin Cancer Res 1998;4:2135–9.
6. Cheung NK, Saarinen UM, Neely JE, et al. Monoclonal antibodies to a glycolipid antigen on human neuroblastoma cells. Cancer Res 1985;45:2642–9.
7. Yu AL, Uttenreuther-Fischer MM, Huang CS, et al. Phase I trial of a human-mouse chimeric anti-disialoganglioside monoclonal antibody ch14.18 in patients with refractory neuroblastoma and osteosarcoma. J Clin Oncol 1998;16:2169–80.
8. Cheung NK, Medof ME, Munn D. Immunotherapy with GD2 specific monoclonal antibodies. Prog Clin Biol Res 1988;271:619–32.
9. Cheung NK, Yeh SD, Gulti S, et al. ^{131}I3F8 targeted radiotherapy of nueroblastoma (NB): a phase I clinical trial. In: Proc Annu Meet Am Assoc Cancer Res; 1990. p. A1686.
10. Livingston PO, Ragupathi G. Carbohydrate vaccines that induce antibodies against cancer. 2. Previous experience and future plans. Cancer Immunol Immunother 1997;45:10–9.
11. Cheung NK, Lazarus H, Miraldi FD, et al. Ganglioside GD2 specific monoclonal antibody 3F8: a phase I study in patients with neuroblastoma and malignant melanoma. J Clin Oncol 1987;5:1430–40.
12. Albertini MR, Hank JA, Schiller JH, et al. Phase IB trial of chimeric antidisialoganglioside antibody plus interleukin 2 for melanoma patients. Clin Cancer Res 1997;3:1277–88.

13. Irie RF, Morton DL. Regression of cutaneous metastatic melanoma by intralesional injection with human monoclonal antibody to ganglioside GD2. Proc Natl Acad Sci U S A 1986;83:8694–8.
14. Saleh MN, Khazaeli MB, Wheeler RH, et al. Phase I trial of the chimeric anti-GD2 monoclonal antibody ch14.18 in patients with malignant melanoma. Hum Antibodies Hybridomas 1992;3:19–24.
15. Saleh MN, Khazaeli MB, Wheeler RH, et al. Phase I trial of the murine monoclonal anti-GD2 antibody 14G2a in metastatic melanoma. Cancer Res 1992;52:4342–7.
16. Cheung NK, Cheung IY, Canete A, et al. Antibody response to murine anti-GD2 monoclonal antibodies: correlation with patient survival. Cancer Res 1994;54: 2228–33.
17. Cheung NK, Guo HF, Heller G, Cheung IY. Induction of Ab3 and Ab3′ antibody was associated with long-term survival after anti-G(D2) antibody therapy of stage 4 neuroblastoma. Clin Cancer Res 2000;6:2653–60.
18. Ragupathi G, Livingston PO, Hood C, et al. Consistent antibody response against ganglioside GD2 induced in patients with melanoma by a GD2 lactone-keyhole limpet hemocyanin conjugate vaccine plus immunological adjuvant QS-21. Clin Cancer Res 2003;9:5214–20.
19. Pirofski LA. Polysaccharides, mimotopes and vaccines for fungal and encapsulated pathogens. Trends Microbiol 2001;9:445–51.
20. May RJ, Beenhouwer DO, Scharff MD. Antibodies to keyhole limpet hemocyanin cross-react with an epitope on the polysaccharide capsule of *Cryptococcus neoformans* and other carbohydrates: implications for vaccine development. J Immunol 2003;171:4905–12.
21. Nussbaum G, Cleare W, Casadevall A, Scharff MD, Valadon P. Epitope location in the *Cryptococcus neoformans* capsule is a determinant of antibody efficacy. J Exp Med 1997;185:685–94.
22. Mukherjee J, Nussbaum G, Scharff MD, Casadevall A. Protective and nonprotective monoclonal antibodies to *Cryptococcus neoformans* originating from one B cell. J Exp Med 1995;181:405–9.
23. Cobb BA, Wang Q, Tzianabos AO, Kasper DL. Polysaccharide processing and presentation by the MHCII pathway. Cell 2004;117:677–87.
24. Cheung NK, Canete A, Cheung IY, Ye JN, Liu C. Disialoganglioside GD2 anti-idiotypic monoclonal antibodies. Int J Cancer 1993;54:499–505.
25. Saleh MN, Stapleton JD, Khazaeli MB, LoBuglio AF. Generation of a human anti-idiotypic antibody that mimics the GD2 antigen. J Immunol 1993;151:3390–8.
26. Basak S, Birebent B, Purev E, et al. Induction of cellular immunity by anti-idiotypic antibodies mimicking GD2 ganglioside. Cancer Immunol Immunother 2003;52:145–54.
27. Cunto-Amesty G, Luo P, Monzavi-Karbassi B, Kieber-Emmons T. Exploiting molecular mimicry: defining rules of the game. Int Rev Immunol 2001;20:157–80.
28. Kieber-Emmons T, Monzavi-Karbassi B, Wang B, Luo P, Weiner DB. Cutting edge: DNA immunization with minigenes of carbohydrate mimotopes induce functional anti-carbohydrate antibody response. J Immunol 2000;165:623–7.
29. Tumilowicz JJ, Nichols WW, Cholon JJ, Greene AE. Definition of a continuous human cell line derived from neuroblastoma. Cancer Res 1970;30:2110–8.
30. Fogh J, Fogh JM, Orfeo T. One hundred and twenty-seven cultured human tumor cell lines producing tumors in nude mice. J Natl Cancer Inst 1977;59:221–6.
31. Pear WS, Nolan GP, Scott ML, Baltimore D. Production of high-titer helper-free retroviruses by transient transfection. Proc Natl Acad Sci U S A 1993;90:8392–6.
32. van Muijen GN, Jansen KF, Cornelissen IM, et al. Establishment and characterization of a human melanoma cell line (MV3) which is highly metastatic in nude mice. Int J Cancer 1991;48:85–91.
33. Mujoo K, Kipps TJ, Yang HM, et al. Functional properties and effect on growth suppression of human neuroblastoma tumors by isotype switch variants of monoclonal antiganglioside GD2 antibody 14.18. Cancer Res 1989;49:2857–61.
34. Smith GP, Scott JK. Libraries of peptides and proteins displayed on filamentous phage. Methods Enzymol 1993;27:228–57.
35. Desai SA, Wang X, Noronha EJ, et al. Structural relatedness of distinct determinants recognized by monoclonal antibody TP25.99 on β 2-microglobulin-associated and β 2-microglobulin-free HLA class I heavy chains. J Immunol 2000;165:3275–83.
36. Sanger F, Nicklen S, Coulson AR. DNA sequencing with chain-terminating inhibitors. Proc Natl Acad Sci U S A 1977;74:5463–7.
37. Altschul SF, Madden TL, Schaffer AA, et al. Gapped BLAST and PSI-BLAST: a new generation of protein database search programs. Nucleic Acids Res 1997;25: 3389–402.
38. Rezacova P, Lescar J, Brynda J, et al. Structural basis of HIV-1 and HIV-2 protease inhibition by a monoclonal antibody. Structure (Camb) 2001;9:887–95.
39. Berman HM, Bhat TN, Bourne PE, et al. The protein data bank and the challenge of structural genomics. Nat Struct Biol 2000;7 Suppl:957–9.
40. Sali A, Blundell TL. Comparative protein modelling by satisfaction of spatial restraints. J Mol Biol 1993;234: 779–815.
41. Cornell WD, Cieplak P, Bayly CI, et al. A second generation force for the simulation of proteins, nucleic acids and organic molecules. J Am Chem Soc 1995;117: 5179–97.
42. Kolinski A, Skolnick J. Assembly of protein structure from sparse experimental data: an efficient Monte Carlo model. Proteins 1998;32:475–94.
43. Feig M, Rotkiewicz P, Kolinski A, Skolnick J, Brooks CL. 3rd Accurate reconstruction of all-atom protein representations from side-chain-based low-resolution models. Proteins 2000;41:86–97.
44. Livingston B, Crimi C, Newman M, et al. A rational strategy to design multiepitope immunogens based on multiple Th lymphocyte epitopes. J Immunol 2002;168: 5499–506.
45. Ahluwalia A, Gokulan K, Nath I, Rao DN. Modification of delivery system enhances MHC nonrestricted immunogenicity of V3 loop region of HIV-1 gp120. Microbiol Immunol 1997;41:779–84.
46. Kieber-Emmons T, Luo P, Qiu J, et al. Vaccination with carbohydrate peptide mimotopes promotes anti-tumor responses. Nat Biotechnol 1999;17:660–5.
47. Batova A, Kamps A, Gillies SD, Reisfeld RA, Yu AL. The Ch14.18-GM-CSF fusion protein is effective at mediating antibody-dependent cellular cytotoxicity and complement-dependent cytotoxicity *in vitro*. Clin Cancer Res 1999;5:4259–63.
48. Winer BJ. Design and analysis of factorial experiments. In: McGraw-Hill, editors. Statistical Principles in Experimental Design. New York: McGraw-Hill; 1971. p. 224–51.
49. Portoukalian J, Carrel S, Dore JF, Rumke P. Humoral immune response in disease-free advanced melanoma patients after vaccination with melanoma-associated gangliosides. EORTC Cooperative Melanoma Group. Int J Cancer 1991;49:893–9.
50. Neal ZC, Yang JC, Rakhmilevich AL, et al. Enhanced activity of hu14.18-IL2 immunocytokine against murine NXS2 neuroblastoma when combined with interleukin 2 therapy. Clin Cancer Res 2004;10:4839–47.
51. Niethammer AG, Xiang R, Ruehlmann JM, et al. Targeted interleukin 2 therapy enhances protective immunity induced by an autologous oral DNA vaccine against murine melanoma. Cancer Res 2001;61: 6178–84.
52. Nakamura K, Hashimoto Y, Yamakawa T, Suzuki A. Genetic polymorphism of ganglioside expression in mouse organs. J Biochem (Tokyo) 1988;103:201–8.
53. Livingston PO, Ritter G, Calves MJ. Antibody response after immunization with the gangliosides GM1, GM2, GM3, GD2 and GD3 in the mouse. Cancer Immunol Immunother 1989;29:179–84.
54. Seyfried TN, Glaser GH, Yu RK. Genetic variability for regional brain gangliosides in five strains of young mice. Biochem Genet 1979;17:43–55.
55. Kawashima I, Nakamura O, Tai T. Antibody responses to ganglio-series gangliosides in different strains of inbred mice. Mol Immunol 1992;29:625–32.